Talanta 88 (2012) 396–402

Contents lists available at SciVerse ScienceDirect

Talanta

journal homepage: www.elsevier.com/locate/talanta

# Fine control of carbon nanotubes–polyelectrolyte sensors sensitivity by electrostatic layer by layer assembly (eLbL) for the detection of volatile organic compounds (VOC)

B. Kumar[a], Y.T. Park[b], M. Castro[a], J.C. Grunlan[b], J.F. Feller[a,*]

[a] *Smart Plastics Group, European University of Brittany (UEB), LIMAT$^B$-UBS, Lorient, France*
[b] *Polymer Nanocomposites Laboratory, Department of Mechanical Engineering, Texas A&M University, College Station, TX, United States*

ARTICLE INFO

*Article history:*
Received 22 July 2011
Received in revised form 27 October 2011
Accepted 1 November 2011
Available online 18 November 2011

*Keywords:*
Vapor sensing
Carbon nanotube
Polyelectrolyte
Conductive architecture
Electrostatic layer by layer (eLbL)
Self-assembly

ABSTRACT

Volatile organic compounds (VOC) sensors have recently extended their field of application to medical area as they are considered as biomarkers in anticipated diagnosis of diseases such as lung cancer by breath analysis. Conductive polymer nanocomposites (CPC) have already proved their interest to fabricate sensors for the design of electronic noses (e-noses) but, for the first time to our knowledge, the present study is showing that electrostatic layer by layer assembly (eLbL) is bringing an interesting input to tailor the sensitivity of carbon nanotubes (CNT)–polyelectrolyte sensors. By this technique transducers are progressively built in 3D alternating dipping into sodium deoxycholate (DOC)-stabilized SWNT and poly(diallyldimethyl-ammonium chloride) [PDDA] solutions, respectively anionic and cationic. The precise control of transducers thicknesses (between 5 and 40 nm) resulting from this process allows a fine tuning of multilayer films resistance (between 50 and 2 kΩ) and thus of their sensitivity to VOC. Interestingly the surfactant used to disperse CNT into water, DOC is also found to enhance CNT sensitivity to vapors so is it for the polyelectrolyte PDDA. Finally it is found that transducers with 16 bilayers of PDDA/DOC-CNT provide optimum chemo-resistive properties for the detection and discrimination of the eight vapors studied (chloroform, acetone, ethanol, water, toluene, dichloromethane, tetrahydrofuran and methanol).

## 1. Introduction

The development of chemical sensor for the detection of volatile organic compound (VOC) is a highly attractive research theme since last two decades [1–33]. Detection of volatile organic vapor molecules and gasses is crucially important for the industrial, environmental and human being safety. With concern to human health, hundreds of organic vapors exist in the exhaled breath of humans. Quantitative as well as qualitative presence of these organic vapors could also be used to identify lung cancer. In addition, organic vapors in human breath are also indicative of other diseases such as, breast cancer, diabetes, several types of liver disease, etc. [29–34]. Since the discovery of one dimensional carbon nanotube (CNT), it has attracted a great deal of attention as CNT are expected to exhibit excellent properties as transducers due to their large surface area and electrical conductivity [1,2,5,8]. Such exceptional characteristics of CNT have been exploited to design chemical sensors in various forms such as field effect transistor (FET) [3,4,22], random networks (RN) [12,14,31,32] and conductive polymer nanocomposites (CPC) [9–11,13–16]. The versatility of their properties by simple adjustment of their formulation, their easy processing in the melt or in solution, the variety of shapes they can take, their operability at room temperature unlike metal oxide based sensors working at several hundred degrees [6,7], make CPC attractive to design multi-sensors able to detect VOC [4,5,9–11,16–19,21,24], explosives [13,15], nerves agent [25,27,28] or to diagnose lung cancer from the presence of biomarkers in patients breath [19,29–33]. Many sensors have been combined together to develop electronic nose. However, discrimination power of e-nose comes from the selectivity of various sensors [23–25]. Therefore, it is crucially important to develop each sensor with a unique sensing pattern. However, some issues such as dispersion of CNT, selectivity of sensors, sensor fabrication and conductive network architecture must be of concern prior to the development of CPC based sensors exhibiting high selectivity as well as fast response. Thus it appears useful to take benefit from tools that proved their effectiveness, first in controlling conducting nanofillers dispersion such as surfactants [35–37], functionalization of filler [8,10,38] and second in structuring a conducting architecture such as decoration [25,26,39], double filler percolation [40], segregated networks [41–44],

---

* Corresponding author. Tel.: +33 297 874 584; fax: +33 297 874 588.
*E-mail address:* jean-francois.feller@univ-ubs.fr (J.F. Feller).

0039-9140/$ – see front matter © 2011 Elsevier B.V. All rights reserved.
doi:10.1016/j.talanta.2011.11.006

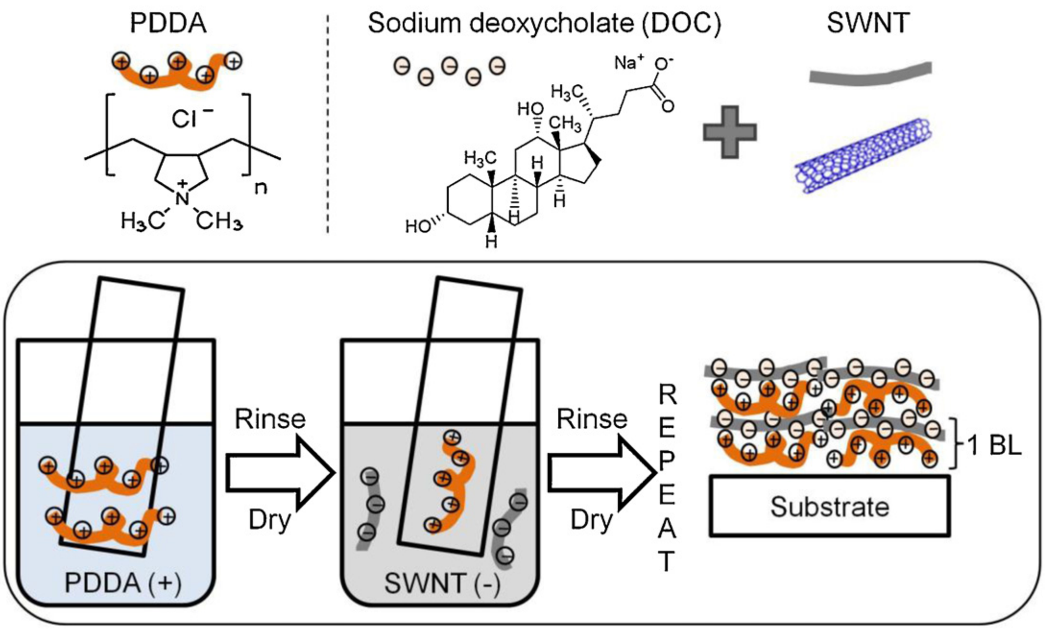

**Fig. 1.** Schematic of the ELbL process for making conductive thin films that involves dipping a substrate in cationic PDDA and anionically stabilized SWNT mixtures, followed by rinsing with water and drying with filtered air. These steps generate one bilayer (BL) and are repeated to grow a film with a given number of bilayers.

self-assembly by electrostatic interactions eLbL [45–57] or spray sLbL [9–11,24,26]. Many of these issues can be evaded using electrostatic layer-by-layer (eLbL) self-assembly, which has been widely used to produce multifunctional thin films in a homogeneous and controlled manner [35,36]. A variety of functional thin films have been produced using the eLbL technique, including antimicrobial, gas barrier, sensing, electrochromic, flame retardant, and electrically conductive eLbL thin films [37,44]. The biggest advantage of this deposition technique is that the number of cycles deposited determines the thickness of the film, thus the final thickness of the coated film can be controlled. Another advantage is the good compatibility with most types and shapes of substrates, such as glass slides, silicon wafers, plastic films (i.e., polyethylene terephthalate (PET), polystyrene and polypropylene), and fabrics [43–47]. In the present work, vapor sensors were assembled by electrostatic layer by layer (eELbL) approach using poly(diallyldimethyl-ammonium chloride) [PDDA] as the polycation, and sodium deoxycholate (DOC)-stabilized SWNT as negatively charged layers. Each positive and negative pair deposited is referred to as a bilayer (BL). Hierarchically structured CPC multilayer films were characterized by transmission electron microscopy (TEM), scanning electron microscopy (SEM) and UV spectroscopy followed by the investigation of their chemo-resistive properties probing the influence of polyelectrolyte characteristics, volatile organic compounds nature and transducer film thickness. To our knowledge it is the first time that a CNT based sensor assembled by eLbL is used to detect VOC, only a couple of works report studies on moisture monitoring [48,49].

## 2. Experimental

### 2.1. Materials

Purified SWNT (1 nm diameter and 0.1–10 μm length, with $C \geq 88$ wt%) were purchased from Unidym Inc. (Menlo Park, CA). Poly(diallyldimethyl-ammonium chloride) (PDDA) with a molecular weight of 100 000–200 000 g $mol^{-1}$, sodium deoxycholate (DOC) ($C_{24}H_{39}NaO_4$, ≥98%), sulfuric acid ($H_2SO_4$, 98%), hydrogen peroxide ($H_2O_2$, 30 vol.%), and methanol (99.8 vol.%) were purchased from Aldrich and used as received. Fused quartz slides (Structure Probe Inc., West Chester, PA), single side polished (1 0 0) silicon wafers (University Wafer, South Boston, MA), and 5 MHz gold electrode quartz crystals (Maxtek, East Syracuse, NY) were used as substrates for visible light absorbance, thickness, and mass measurements, respectively. Poly(ethylene terephthalate) PET (0.175 mm Melinex ST505) was purchased from Tekra Corp., New Berlin, WI. Substrates were cut to size for TEM and SEM images.

### 2.2. Electrostatic layer-by-layer assembly

A 0.25 wt% PDDA aqueous solution was prepared as a cationic solution. The anionic solution was prepared by dissolving 0.05 wt% SWNT in deionized water, stabilized by 1 wt% DOC and followed by mild ultrasonication for 20 min to remove large SWNT bundles and impurities. All quartz slides and silicon wafers were prepared by piranha treatment. The quartz slides were treated with a PDC 32G oxygen plasma etcher (Harrick Plasma, Ithaca, NY) prior to use. PET substrates were cleaned with methanol, followed by rinsing, drying, and corona treatment with a BD-20C Corona treater (Electro-Technic Products, Inc., Chicago, IL). Each eLbL deposition was proceeded by alternately immersing into the PDDA solution and DOC-stabilized SWNT suspension, rinsing with deionized water, and drying with filtered air as schemed in Fig. 1. Following deposition, all films were stored in a dry box for a minimum of 12 h prior to testing. The detailed procedures for eLbL assemblies are described in a previous publication [57]. PDDA/DOC-CNT samples were prepared following the same eLbL deposition technique on top of interdigitated copper electrodes (IDE) that had been etched by photolithography on epoxy substrate and cleaned in ethanol. Typical dimensions of IDE were (10 mm × 10 mm × 2 mm) with track gap and width of 0.5 mm of 0.25 mm, respectively (see IDE photo in Fig. 2). Beforehand, in order to investigate the effect of DOC on the chemo-resistive properties, neat CNT and CNT-DOC solutions were prepared; CNT (2 mg) were dispersed in chloroform (20 $cm^3$) via sonication (30 min). The DOC-CNT solution was prepared separately by dispersing CNT (2 mg) in aqueous solution of DOC (0.5 wt% in 20 $cm^3$). The CNT and CNT-DOC solutions were respectively deposited onto cleaned electrodes (IDE) via solution

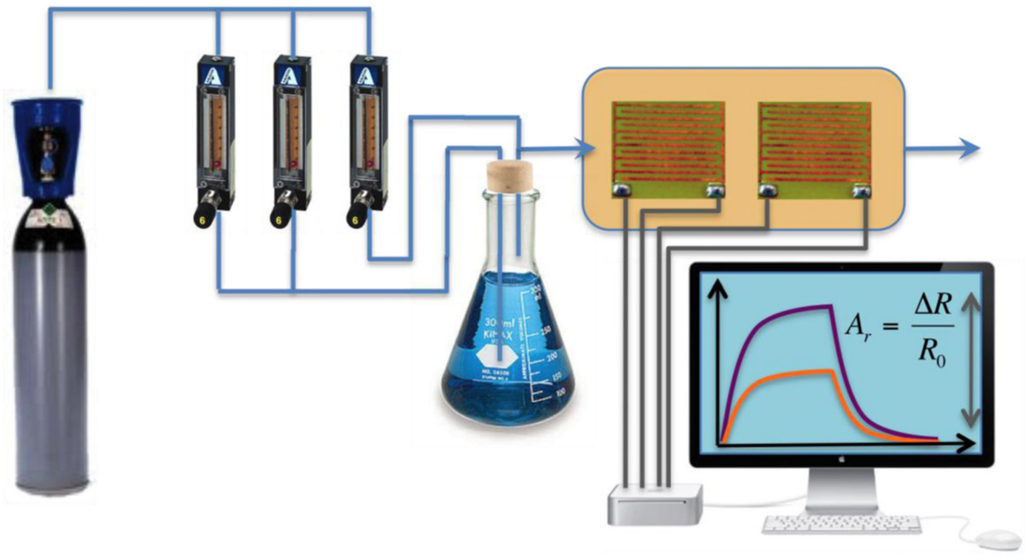

**Fig. 2.** Scheme of chemo-resistive vapor sensing device [42].

spraying technique [11], with a homemade device allowing a precise control of nozzle scanning speed (Vs = 10 cm $s^{-1}$), solution flow rate (index 2), stream pressure (ps = 0.20 MPa), and target to nozzle distance (dtn = 8 cm).

### 2.3. Characterization techniques

#### 2.3.1. Thin multilayer film characterization

Thickness data was obtained with a PHE-101 Ellipsometer (Microphonics, Allentown, PA) with a 632.8 nm laser and using a 65° angle of incidence. The weight was measured with a Maxtek (East Syracuse, NY) research quartz crystal microbalance (QCM) by dipping the entire crystal and holder into each deposition mixture. Absorbance of films on quartz slides was measured between 250 and 850 nm with a USB2000 UV-vis spectrometer (Ocean Optics, Dunedin, FL). Thin film cross-section images were obtained with a Jeol 1200 EX TEM (Jeol USA Inc., Peabody, MA) with an operating voltage of 100 kV. TEM specimens were embedded in an epoxy resin comprised of Araldite 502 modified bisphenol A and Quetol 651 ethylene glycol diglycidyl ether, along with dodecenyl succinic anhydride hardener (2:1:1 mole ratio) and benzyl dimethyl amine accelerator (0.02 ml per 1 g of total epoxy resin). The specimens were sectioned and placed on 300 mesh nickel grids. Surface images were obtained with a Quanta 600 FE-SEM (FEI Co., Hillsboro, OR) at an operating voltage of 100 kV.

### 2.4. Dynamical vapor sensing measurement

Chemo-resisitive properties of PDDA/DOC-CNT sensors were investigated by recording their electrical responses when submitted to 10 min successive cycles of dry nitrogen and vapors streams. The dynamic system consisting in mass flow controllers, solvent bubblers and electrical valves is controlled by LabView software. Bubbling dry nitrogen in liquid solvent provides a saturated vapor stream, which can in turn be diluted by dry nitrogen flow to the desired concentration at room temperature. In this paper we did not vary the concentration of vapors to study the influence of this parameter on chemo-resistive properties of sensors, but this has been already done in previous works by using the LHC model, which predicts the concentration dependency of electrical responses [9,11,24]. Moreover, the limit of detection (LOD) of our systems is in the range of 2–10 ppm, which is compatible with the necessity to detect ppb concentrations of VOC in breath, provided that a preconcentrator is used. The sensing device [42] is presented in Fig. 2 and samples were placed in 90 mm × 10 mm × 3.5 mm chamber. The total flow rate was kept constant at $Q_v = 100\,cm^3\,min^{-1}$. Electrical characteristics of the CPC transducer were recorded with a Keithley 6517A multimeter.

## 3. Results and discussion

### 3.1. Growth of SWNT assemblies

Morphological characterizations of eLbL assemblies were done with different types of electronic microscopes requiring specific substrates. Nevertheless the multilayer deposition was done in the same way as for transducers association to interdigitated electrodes. Fig. 3a shows an image of a series of SWNT-based assemblies denoted as $[PDDA/(SWNT\text{-}DOC)]_n$, where $n$ is the number of bilayers deposited. A TEM micrograph of this film's cross-section, which illustrates a highly inter-diffused nanostructure, is shown in Fig. 3b. Dark and light grey areas are SWNT-rich and PDDA-rich regions, respectively, and the darkest black spots are catalyst impurities. The uniform distribution of SWNT in the matrix is due to the effectiveness of DOC as a stabilizer for SWNT [35,36]. In addition to highlighting thin films structure, the TEM image verifies the 38.4 nm thickness of a $[PDDA/(SWNT\text{-}DOC)]_{20}$ film, measured independently by ellipsometry. The surfaces of these SWNT-based assemblies were also analyzed using SEM, as shown in Fig. 3c. A surface image of $[PDDA/(SWNT\text{-}DOC)]_{20}$ shows a homogeneous network of SWNT. DOC exfoliation of individual SWNT in water ultimately forms a uniform distribution in the thin film. SWNT contacts within this network offer a pathway for electron transport through the film, as shown in these SEM images (as well as in the TEM image in Fig. 3b). Growth of this film proceeds at 1.9 nm per BL, which suggests very uniform deposition of highly individualized SWNT. Linear growth of these nanotube-based thin films up to 20 BL was observed using several complementary techniques (ellipsometry for thickness, quartz crystal microbalance (QCM) for mass, and UV–vis absorbance), as shown in Fig. 4a. The constant concentration of SWNT in every bilayer, determined with QCM, supports the assumption that the increasing absorbance of $[PDDA/(DOC\text{-}CNT)]_n$ is due to increasing film thickness. Linear growth also confirms successful combination of positively and negatively charged components and constant composition up to 20 BL. Fig. 4b shows the absorbance and transmittance spectra of the $[PDDA/(DOC\text{-}CNT)]_n$

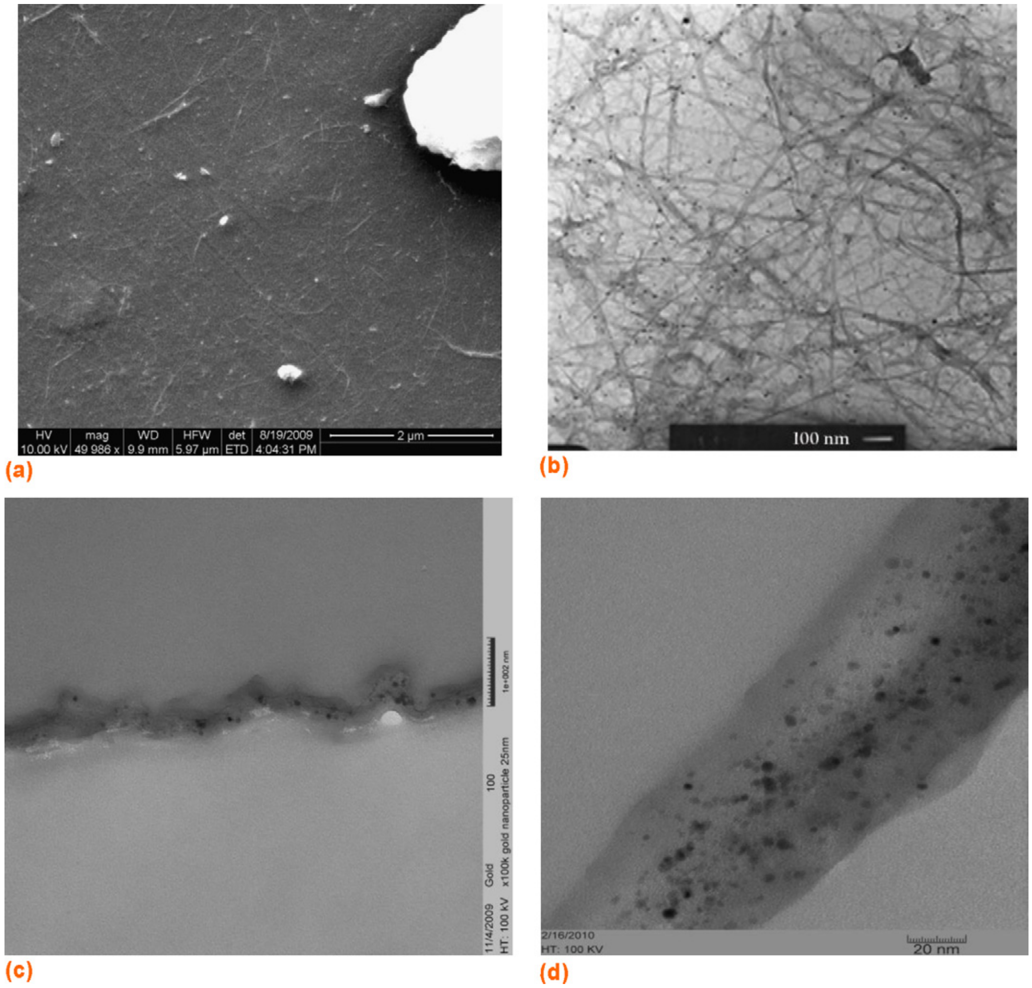

**Fig. 3.** (a) SEM image for PDDA/DOC-CNT (4 BL), (b) dispersion of CNT (TEM image), (c) thickness of PDDA/DOC-CNT (20 BL) and (d) high resolution image for thickness measurement.

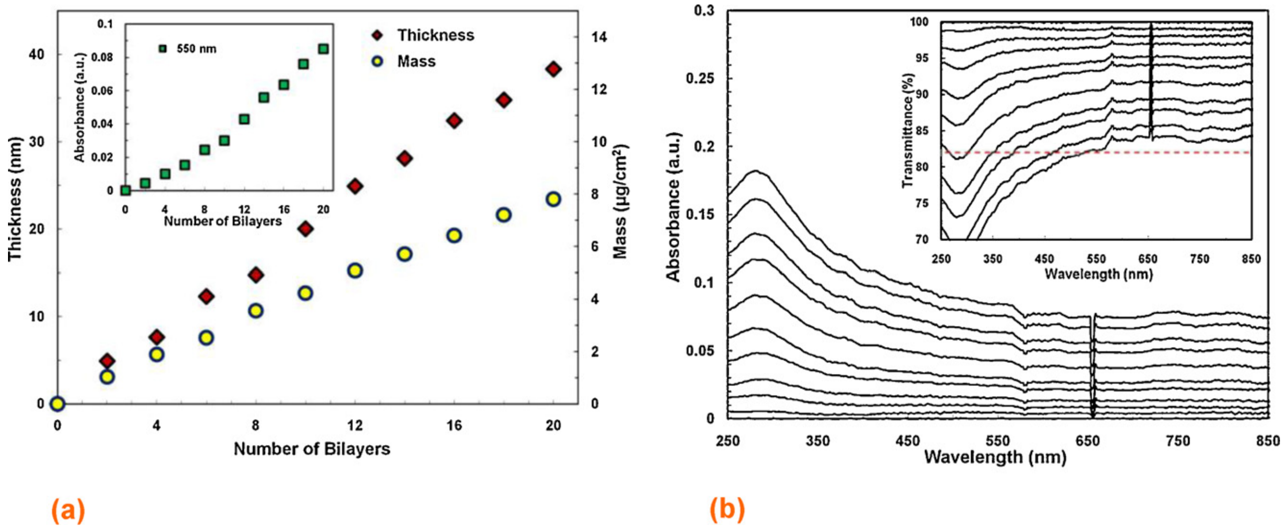

**Fig. 4.** (a) Growth of PDDA/(SWNT-DOC) thin films, as a function of the number of bilayers deposited. Film thickness was obtained by ellipsometry, mass by QCM, and absorbance (at 550 nm) by UV–vis (inset), respectively. (b) Absorbance and transmittance spectra of PDDA/(SWNT-DOC) thin films, measured in 2 BL step up to 20 BLs by the UV–vis spectrometer.

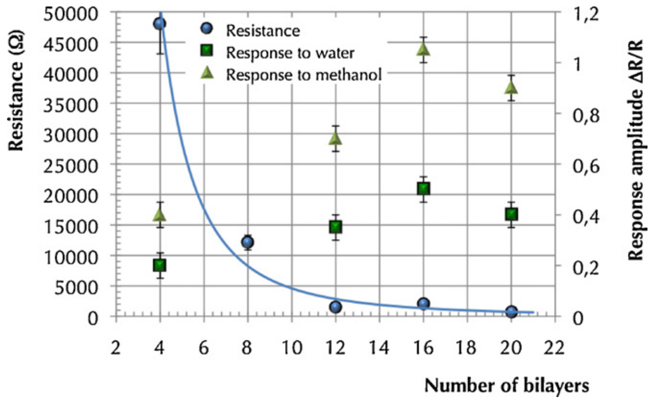

**Fig. 5.** Electrical resistance change as a function of deposited bilayers. Measurement was performed on PDDA/(SWNT-DOC) deposited on interdigitated electrodes.

films between 300 and 850 nm, up to 20 bilayers. The PDDA/(DOC-CNT) system has over 82% transmittance with 20 bilayers and over 98% with only two bilayers at 550 nm wavelength. An increasing number of PDDA/(DOC-CNT) bilayers was deposited on interdigitated electrodes and electrical resistance were measured. Close packing of this layered structure resulted in an electrical resistance decrease, as illustrated in Fig. 5. While thickness increase and mass uptake as a function of bilayers number revealed a linear growth, electrical resistance of the system exhibited a power law decrease as could be expected for percolated systems.

## 3.2. Vapor sensing properties of PDDA/DOC-CNT transducers

### 3.2.1. Influence of DOC on chemo-resistive properties

Before investigating the sensing behavior of PDDA/(DOC-CNT) multilayer system, we have been wondering whether DOC could not influence CNT selectivity or sensitivity towards VOC. For that purpose, a surfactant free deposition process was chosen to make the sensors, namely spray layer by layer technique (described in Section 2). Thus it was possible to fabricate transducers made of five monolayers of CPC onto the same interdigitated electrodes as that used for electrostatic LbL. Sensors made by deposition of CNT in chloroform without any surfactant and CNT stabilized with DOC in water were exposed to the same standard set of solvents vapors (chloroform, acetone, ethanol, water and toluene). The resistance changes recorded during experiments were converted into relative amplitude $A_r$, calculated from Eq. (1), which allows comparisons the sensor's performances:

$$A_r = \frac{R_v - R_{ini}}{R_{ini}} \qquad (1)$$

where $R_v$ is the resistance of sensor when exposed to vapor and $R_{init}$ is the initial resistance in dry nitrogen at room temperature.

Fig. 6 shows that DOC molecules have a limited influence on CNT selectivity towards solvent vapors, but strongly enhance their sensitivity, i.e., double the amplitude of their responses to almost all solvents, excepted that of acetone which is only slightly larger. Therefore, it can be concluded that the use of DOC surfactant has positive effect on the sensors chemo-resistive characteristics, mainly by improving CNT dispersion (see Fig. 3b) and thus the total surface accessible to vapor molecules.

## 3.3. Chemo-resistive behavior of $[PDDA/(DOC\text{-}CNT)]_{16}$

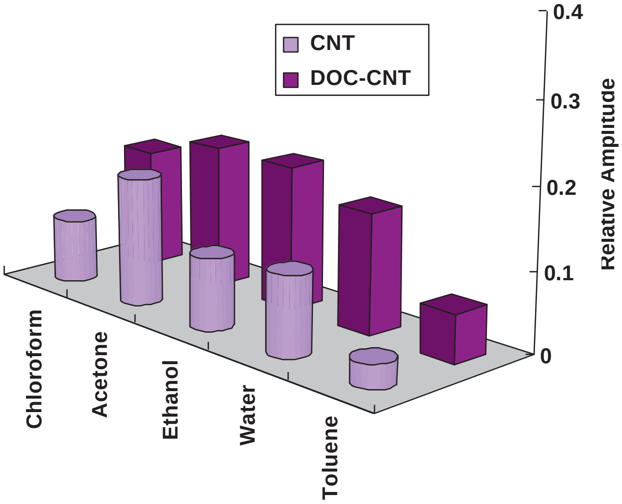

**Fig. 6.** Influence of DOC on sensing characteristics of SWNT deposited on interdigitated electrodes.

Coming back to the investigation of the multilayer transducer chemo-resistive behavior, $[PDDA/(DOC\text{-}CNT)]_{16}$ sensors were exposed to a set of analytes representative of the variety of VOC (concentration of 100%), comprising the vapors studied in previous paragraph, i.e., chloroform, **acetone**, **ethanol**, water and **toluene** (vapors in bold caps are part of lung cancer biomarkers according to authors of Refs. [30,31,34]), plus three additional ones, dichloromethane, tetrahydrofuran and **methanol**. The choice of transducers made of 16 bilayers is justified by the fact that it corresponds to the optimum of response amplitude to water and methanol as shown in Fig. 5. The first comments about signals collected in Fig. 7, are that responses are fast (only some seconds are needed to get a measurable variation of resistance), reversible (the recovery of initial resistance shows that analyte molecules are not kept inside the transducer) and reproducible (first and second cycles are almost identical suggesting that the conducting network structure has not been modified) for all vapors. These results suggest that the eLbL process provides a conductive CNT networks able on the one hand to easily disconnect/reconnect itself upon vapor molecules diffusion due to its weak thickness, and on the other hand to be enough robust to support local swelling by VOC thanks to a close packing of layers by electrostatic assembly. The second aspect to be considered is the ability of sensors to discriminate between the different vapors to which it is submitted. Actually, the comparison of responses maximal amplitude $A_{r\,max}$ for each analyte after 10 min exposure in Fig. 7, reveals the following ranking: $A_r$(methanol) > $A_r$(ethanol) > $A_r$(dichloromethane) >

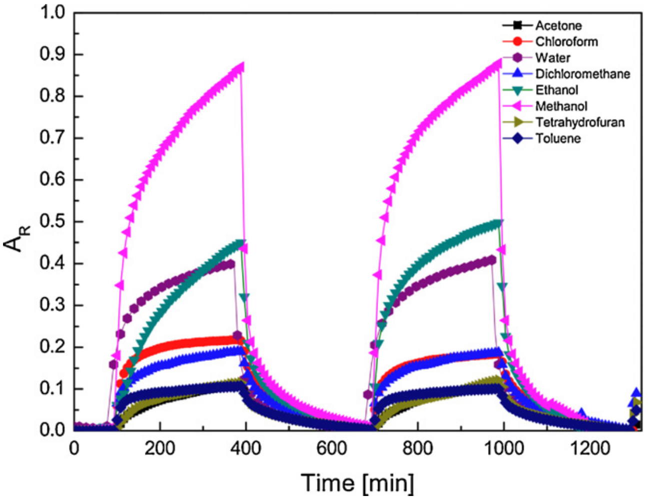

**Fig. 7.** Chemo-resistive signal of $[PDDA/(DOC\text{-}CNT)]_{16}$ towards studied vapors.

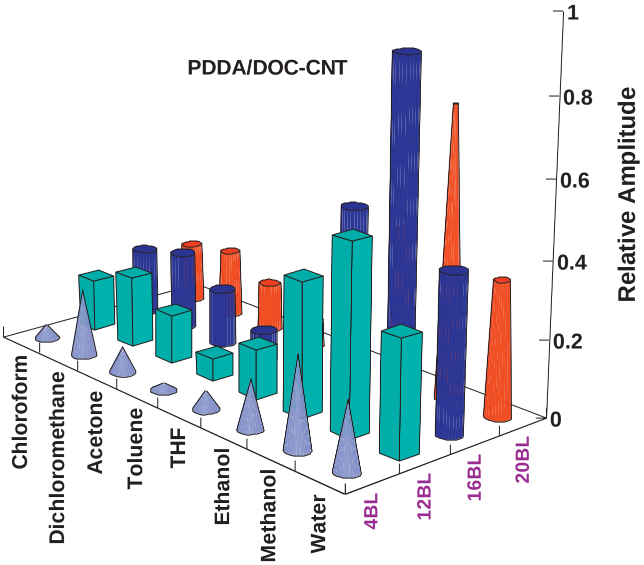

**Fig. 8.** Vapor sensing pattern of PDDA/(DOC-CNT) multilayer conductive polymer nanocomposites.

$A_\mathrm{r}$(chloroform) > $A_\mathrm{r}$(tetrahydrofuran) > $A_\mathrm{r}$(acetone) > $A_\mathrm{r}$(toluene). Moreover vapors can be associated by families, alcohols > chlorinated solvents > cyclic molecules and acetone demonstrating the good selectivity of [PDDA/(DOC-CNT)]$_{16}$ sensors.

### *3.4. Influence of number of layers on selectivity and sensitivity of sensors towards VOC*

In order to have an overview of both sensitivity and selectivity of [PDDA/(DOC-CNT)]$_n$ sensors as a function of $n$, the number of bilayers of the transducer, the maximum amplitudes of all sensors responses after 10 min exposure to the eight solvent vapors studied have been summarized in Fig. 8. This graph highlights that there is a compromise to find between electrical conductivity of the multilayer film (driven by the number of layers) and it sensitivity function of it ability to give a quick and large response (driven by the vicinity to the percolation threshold), without compromising the reproducibility of the signals in time (only small distance variations, of the order of some nm, are allowed at CNT/CNT junctions). It is also striking that although the 4 BL transducer is the less sensitive of the series, it gives measurable signals which selectivity (ranking of amplitude to vapors) is the same as the most sensitive ones. This means that transparent vapor sensors could be designed by eLbL process, as 4 BL only correspond to 8 nm thick transducers.

## 4. Conclusion

The electrostatic layer by layer assembly (eLbL) process was found to bring an interesting input to the field of Conductive polymer nanocomposites (CPC) vapor sensors as it provides transducers with high stability due to the progressive building in 3D of alternating anionic and cationic nanolayers. The precise control of transducers thicknesses allows a fine tuning of multilayer films resistance and thus of their sensitivity to VOC. Its has been showed that both DOC the surfactant used to disperse CNT into water, and the cationic polyelectrolyte PDDA were enhancing CNT sensitivity to VOC. Finally it is the transducers with 16 bilayers of PDDA/DOC-CNT which are found to provide optimum chemo-resistive properties for the detection and discrimination of the eight vapors studied (chloroform, acetone, ethanol, water, toluene, dichloromethane, tetrahydrofuran and methanol). Thus it is likely that eLbL technique will have a strong potential of development in the fabrication of highly sensitive vapor sensors.

## Acknowledgments

The authors are grateful to Hervé BELLEGOU for his contribution to this work. This research was financed by NSF grant DBI-0116835, the VP for Research Office, and the Texas Engineering Experiment Station together with INTELTEX European Integrated Project supported through the Sixth Framework Program for Research and Technological Development of European Commission (NMP2-CT-2006-026626).

## References

[1] P.G. Collins, K. Bradley, M. Ishigami, A. Zettl, Science 287 (2000) 1801–1804.
[2] J. Kong, N.R. Franklin, C. Zhou, M.G. Chapline, S. Peng, K. Cho, H. Dai, Science 287 (2000) 622–625.
[3] A. Star, T.R. Han, J.C.P. Gabriel, K. Bradley, G. Grüner, Nano Lett. 3 (10) (2003) 1421–1423.
[4] T. Someya, J. Small, P. Kim, C. Nuckolls, J.T. Yardley, Nano Lett. 3 (7) (2003) 877–881.
[5] J. Li, Y. Lu, Q. Ye, M. Cinke, J. Han, M. Meyyappan, Nano Lett. 3 (7) (2003) 929–933.
[6] C. Wongchoosuk, A. Wisitsoraat, A. Tuantranont, T. Kerdcharoen, Sens. Actuators B: Chem. 147 (2010) 392–399.
[7] N. Bahadur, K. Jain, R. Pasricha, S. Govind, Chand, Sens. Actuators B: Chem. 159 (2011) 112–120.
[8] I. Sayago, H. Santos, M.C. Horrillo, M. Aleixandre, M.J. Fernández, E. Terrado, I. Tacchini, R. Aroz, W.K. Maser, A.M. Benito, M.T. Martínez, J. Gutiérrez, E. Munoz, Talanta 77 (2008) 758–764.
[9] J. Lu, B. Kumar, M. Castro, J.F. Feller, Sens. Actuators B: Chem. 140 (2009) 451–460.
[10] M. Castro, J. Lu, S. Bruzaud, B. Kumar, J.F. Feller, Carbon 47 (2009) 1930–1942.
[11] B. Kumar, J.F. Feller, M. Castro, J. Lu, Talanta 81 (2010) 908–915.
[12] C. Staii, A.T. Johnson, M. Chen, A. Gelperin, Nano Lett. 5 (2005) 1774–1778.
[13] J. Yinon, Anal. Chem. 3 (2003) 99–105.
[14] J.A. Robinson, E.S. Snow, F.K. Perkins, Sens. Actuators B: Chem. 135 (2007) 309–314.
[15] A. Diaz Aguilar, E.S. Forzani, M. Leright, F. Tsow, A. Cagan, R.A. Iglesias, L.A. Nagahara, I. Amlani, R. Tsui, N.J. Tao, Nano Lett. 10 (2010) 380–384.
[16] M.C. Lonergan, E.J. Severin, B.J. Doleman, S.A. Beaber, R.H. Grubbs, N.S. Lewis, Chem. Mater. 8 (9) (1996) 2298–2312.
[17] K.J. Albert, N.S. Lewis, C.L. Schauer, G.A. Sotzing, S.E. Stitzel, T.P. Vaid, D.R. Walt, Chem. Rev. 100 (2000) 2595–2626.
[18] N.S. Lewis, Acc. Chem. Res. 37 (9) (2004) 663–672.
[19] N.K. Kang, T.S. Jun, D.D. La, J.H. Oh, Y.W. Cho, Y.S. Kim, Sens. Actuators B: Chem. 147 (2010) 55–60.
[20] C.K.W. Adu, G.U. Sumanasekera, B.K. Pradhan, H.E. Romero, P.C. Eklund, Chem. Phys. Lett. 337 (1–3) (2001) 31–35.
[21] J. Janata, M. Josowicz, Nat. Mater. 2 (2002) 19–24.
[22] A. Saheb, M. Josowicz, J. Janata, Anal. Chem. 80 (2008) 4214–4219.
[23] O.S. Kwon, E. Park, O.Y. Kweon, S.J. Park, J. Jang, Talanta 82 (2010) 1338–1343.
[24] J. Lu, B.J. Park, B. Kumar, M. Castro, H.J. Choi, J.F. Feller, Nanotechnology 21 (2010) 255501, pp. 1–10.
[25] P. Poonam, N. Deo, Sens. Actuators B: Chem. 135 (2008) 327–335.
[26] J.F. Feller, J. Lu, K. Zhang, B. Kumar, M. Castro, N. Gatt, H.J. Choi, J. Mater. Chem. 21 (2011) 4142–4149.
[27] Y. Wang, Z. Zhou, Z. Yang, X. Chen, D. Xu, Y. Zhang, Nanotechnology 20 (2009) 345502, pp. 1–8.
[28] L. Kong, J. Wang, X. Fu, Y. Zhong, F. Meng, T. Luo, J. Liu, Carbon 48 (2010) 1262–1270.
[29] A.P.F Turner, N. Magan, Nat. Rev. Microbiol. 2 (2004) 161–166.
[30] G. Peng, E. Trock, H. Haick, Nano Lett. 8 (11) (2008) 3631–3635.
[31] G. Peng, U. Tisch, H. Haick, Nano Lett. 9 (4) (2009) 1362–1368.
[32] H. Haick, M. Hakim, M. Patrascu, C. Levenberg, N. Shehada, F. Nakhoul, Z. Abassi, ACS Nano 3 (5) (2009) 1258–1266.
[33] G. Peng, M. Hakim, Y.Y. Broza, S. Billan, R. Abdah-Bortnyak, A. Kuten, U. Tisch, H. Haick, Br. J. Cancer 103 (2010) 542–551.
[34] R.F. Machado, D. Laskowski, O. Deffenderfer, T. Burch, S. Zheng, P.J. Mazzone, T. Mekhail, C. Jennings, J.K. Stoller, J. Pyle, J. Duncan, R.A. Dweik, S.C. Erzurum, Am. J. Resp. Crit. Care Med. 171 (2005) 1286–1291.
[35] X. Gong, J. Liu, S. Baskaran, R.D. Voise, J.S. Young, Chem. Mater. 12 (2000) 1049–1052.
[36] N. Grossiord, J. Loos, O. Regev, C.E. Koning, Chem. Mater. 18 (5) (2006) 1089–1099.
[37] L. Vaisman, G. Marom, H.D. Wagner, Adv. Funct. Mater. 16 (2006) 357–363.
[38] H. Zeng, C. Gao, D. Yan, Adv. Funct. Mater. 16 (2006) 812–818.
[39] M.A. Correa-Duarte, A. Kosiorek, W. Kandulski, M. Giersig, L.M. Liz-Marzn, Chem. Mater. 17 (12) (2005) 3268–3272.
[40] L. Liu, J.C. Grunlan, Adv. Funct. Mater. 17 (2007) 2343–2348.

[41] J.C. Grunlan, A.R. Mehrabi, M.V. Bannon, J.L. Bahr, Adv. Mater. 16 (2) (2004) 150–153.
[42] J. Lu, J.F. Feller, B. Kumar, M. Castro, Y.S. Kim, Y.T. Park, J.C. Grunlan, Sens. Actuators B: Chem. 155 (2011) 28–36.
[43] M.O. Lisunova, Y.P. Mamunya, N.I. Lebovka, A.V. Melezhyk, Eur. Polym. J. 4 (2007) 949–958.
[44] P. Bertrand, A. Jonas, A. Laschewsky, R. Legras, Macromol. Rapid Commun. 21 (7) (2000) 319–348.
[45] P.T. Hammond, Adv. Mater. 16 (15) (2004) 1271–1293.
[46] S.Y. Wong, Q. Li, J. Veselinovic, B.S. Kim, A.M. Klibanov, P.T. Hammond, Biomaterials 31 (14) (2010) 4079–4087.
[47] M.A. Priolo, D.J. Gamboa, C. Grunlan, ACS Appl. Mater. Interfaces 2 (1) (2010) 312–320.
[48] H. Yu, T. Cao, L. Zhou, E. Gu, D. Yu, D. Jiang, Sens. Actuators B: Chem. 119 (2006) 512–515.
[49] L. Liu, X. Ye, K. Wu, Z. Zhou, D. Lee, T. Cui, IEEE Sens. J. 9 (10) (2009) 1308–1314.
[50] K.J. Loh, J. Kim, J.P. Lynch, N.W.S. Kam, N.A. Kotov, Smart Mater. Struct. 16 (2) (2007) 429–438.
[51] Y.T. Park, J.C. Grunlan, Electrochim. Acta 55 (9) (2010) 3257–3267.
[52] Y.C. Li, J. Schulz, S. Mannen, C. Delhom, B. Condon, S. Chang, M. Zammarano, J.C. Grunlan, ACS Nano 4 (6) (2010) 3325–3337.
[53] B.S. Shim, Z.Y. Tang, M.P. Morabito, A. Agarwal, H.P. Hong, N.A. Kotov, Chem. Mater. 19 (23) (2007) 5467–5474.
[54] H.J. Park, K.A. Oh, M. Park, H. Lee, J. Phys. Chem. C 113 (30) (2009) 13070–13076.
[55] J.L. Lutkenhaus, K.D. Hrabak, K. McEnnis, P.T. Hammond, J. Am. Chem. Soc. 127 (49) (2005) 17228–17234.
[56] M. Agarwal, Y. Lvov, K. Varahramyan, Nanotechnology 17 (21) (2006) 5319–5325.
[57] Y.C. Li, J. Schulz, J.C. Grunlan, ACS Appl. Mater. Interfaces 1 (10) (2009) 2338–2347.